Accepted Manuscript

Simultaneous chemosensing of tryptophan and the bacterial signal molecule indole by boron doped diamond electrode

Alyah Buzid, F. Jerry Reen, Fergal O'Gara, Gerard P. McGlacken, Jeremy D. Glennon, John H.T. Luong

PII: S0013-4686(18)31393-8

DOI: 10.1016/j.electacta.2018.06.105

Reference: EA 32098

To appear in: *Electrochimica Acta*

Received Date: 20 March 2018

Revised Date: 13 June 2018

Accepted Date: 14 June 2018

Please cite this article as: A. Buzid, F.J. Reen, F. O'Gara, G.P. McGlacken, J.D. Glennon, J.H.T. Luong, Simultaneous chemosensing of tryptophan and the bacterial signal molecule indole by boron doped diamond electrode, *Electrochimica Acta* (2018), doi: 10.1016/j.electacta.2018.06.105.

Simultaneous Chemosensing of Tryptophan and the Bacterial Signal Molecule Indole by Boron Doped Diamond Electrode

Alyah Buzid [a,b], F. Jerry Reen [c], Fergal O'Gara [d,e], Gerard P. McGlacken [b], Jeremy D. Glennon [a,b,*], and John H. T. Luong [a,b,*]

[a] Innovative Chromatography Group, Irish Separation Science Cluster (ISSC) Ireland, University College Cork, Cork, Ireland

[b] School of Chemistry and Analytical & Biological Chemistry Research Facility (ABCRF), University College Cork, College Road, Cork T12 YN60, Ireland

[c] School of Microbiology, University College Cork, College Road, Cork T12 YN60, Ireland

[d] BIOMERIT Research Centre, School of Microbiology, University College Cork, College Road, Cork T12 YN60, Ireland

[e] School of Biomedical Sciences, Curtin Health Innovation Research Institute, Curtin University, Perth WA 6845, Australia

* Corresponding authors:

E-mail address: j.glennon@ucc.ie (J. D. Glennon) and j.luong@ucc.ie (J. H. T. Luong)

ABSTRACT

A simple and robust chemosensing approach using a boron-doped diamond (BDD) electrode has been developed and applied to analyze tryptophan (TRP) and indole during the growth of *Escherichia coli* in a complex growth medium. The bacterial enzyme tryptophanase catalyzes TRP to indole, an emerging signaling molecule. The process can now be monitored using electrochemistry, in a method far beyond the traditional identification protocols. Electroanalysis in a non-aqueous medium comprising acetonitrile (ACN) and tetrabutylammonium hexafluorophosphate (TBAH) is capable of separating the oxidation peak of TRP from that of indole. Mechanisms are postulated for the electrochemical oxidation of indole and TRP in ACN chosen because of its wider potential range, proton acceptor property, and solubilization of analytes. The electrochemical oxidation of TRP involves the elimination of two electrons. With a detection limit of 0.5 µM for both indole and TRP, this chemosensing approach is sufficient to monitor the level of these two biomolecules during the bacterial growth period.

Keywords:

Indole; tryptophan; boron-doped diamond electrode; electrochemical detection; *Escherichia coli*

1. Introduction

The indole moiety is a ubiquitous heterocyclic compound found in several natural products and synthetic compounds [1], including the non-steroidal anti-inflammatory indomethacin, and the anti-HIV drug delavirdine. Over 85 different gram-positive and gram-negative bacteria synthesize a significant amount of indole. As an example, tryptophanase, a cytoplasmic enzyme of *Escherichia coli* hydrolyzes tryptophan (TRP) to indole, pyruvate, and ammonia [2]. This biomolecule has been implicated in biofilm formation, virulence, and antibiotic resistance [3-7]. The essential amino acid TRP is an important precursor of hormones, melatonin, vitamins, niacin, neurotransmitters, and serotonin [8, 9]. Low plasma concentrations of TRP can be linked to insomnia, anxiety, and depression. Indole acts as an extracellular signaling molecule [7], present in the human gastrointestinal tract, which triggers responses in bacteria [10]. The *E. coli* indole signal increases epithelial-cell tight-junction resistance and attenuates indicators of inflammation.

High-performance liquid chromatography (HPLC) and gas chromatography (GC) are commonly used for accurate measurement of indole and TRP in beverage and biological samples [11-13]. In addition to the complexity of special equipment, chromatographic analysis of TRP in protein hydrolysates is more challenging as it is destroyed by acid hydrolysis, even under optimal conditions used with other amino acids. These expensive and labor-intensive methods are lab-based and not well suited to routine or spot analysis.

Levels of indole and its analogs in biological samples can be estimated using the simple and rapid Kovac's assay [4]. The commercially available Kovac's or Ehrlich's reagent consists of isoamyl alcohol, *para*-dimethylaminobenzaldehyde (DMAB), and concentrated hydrochloric acid. The indole reacts with DMAB to yield a red complex, which is used to differentiate *E. coli* from other indole-negative bacteria, e.g., *Pseudomonas aeruginosa* [13]. However, the reaction color changes from pink to yellowish orange at high indole concentrations, reducing the absorption maxima at 530 nm and thus the quantitation

accuracy. Evidently, a fast and accurate general method for simultaneous analysis of TRP and indole in complex biological matrices is of importance for diversified applications, whereas both HPLC and GC still play an important role as routine standard methods. Although considerable efforts have been expended to develop electrochemical sensing for TRP, its voltammetric response is not satisfactory due to the slow heterogeneous electron transfer. Also, modified electrodes for TRP are still limited and suffer from poor reproducibility.

The boron-doped diamond (BDD) electrode is of particular importance for the analysis of target analytes with limited aqueous solubility and oxidation potentials over + 1V [14-19] and thus demonstrates potential as a basis for a novel sensing methodology for indole, TRP, and their analogs. The single electrochemical detection of indole or TRP using the BDD electrode was previously reported [20-22]. In this paper, we describe a chemosensing protocol for quantitating TRP and indole in the most commonly used growth medium for *E. coli*, using a bare BDD electrode. The detection is performed in a non-aqueous milieu, containing an organic conducting salt, to alleviate electrode fouling due to the non-specific adsorption of diversified biomolecules of the growth medium. This non-aqueous sensing protocol also circumvents the subsequent oxidation and electrode surface fouling, arising due to oxidized products stemming from TRP and indole. The simultaneous detection of TRP and indole is successfully achieved in a non-aqueous media consisting of 0.2 M tetrabutylammonium hexafluorophosphate in acetonitrile (TBAH/ACN). It is noteworthy that the simultaneous detection of both target analytes proved unsuccessful in aqueous media. The proposed method is assessed for its analytical performance and reproducibility, and a limit of detection (LOD) is established. Application of the method was then demonstrated using a growth medium of *E. coli*, as a relevant model study. Here, metabolization of TRP to indole was monitored and quantified during bacterial growth.

2. Experimental

2.1 Chemicals

Sodium phosphate monobasic, sodium phosphate dibasic, phosphoric acid, indole, tryptophan (TRP), sodium hydroxide, potassium chloride, potassium hexacyanoferrate, acetonitrile (ACN), methanol (CH_3OH). Kovac's reagent for indoles, tetrabutylammonium hexafluorophosphate (TBAH), and ethanol were purchased from Sigma-Aldrich (Dublin, Ireland). 50 mM phosphate buffer solutions were prepared at pH 2 and pH 7 with ACN (80: 20, v/v) were used as aqueous buffers. ACN was used to support the solubility of the target analytes. The stock solution of indole (2 mM) were prepared in ACN daily before use, while the stock solution of TRP was prepared in CH_3OH: H_2O (70: 30, v/v) at 2 mM. Deionized water (Millipore, Ireland) was utilized throughout the experiments, and all chemicals were of the analytical grade.

2.2 Apparatus and measurements

All measurements were performed at room temperature using a CHI1040A electrochemical workstation (CH Instrument, Austin, TX). The electrochemical cell consists of the BDD working electrode (Windsor Scientific, Slough Berkshire, UK), a Pt wire counter electrode (Sigma-Aldrich, Dublin, Ireland), and a silver/silver chloride (Ag/AgCl /3M KCl) reference electrode (BAS Analytical Instruments, West Layette, IN). The BDD electrode was polished using 0.3 and 0.05 µm alumina slurry with wet Nylon and MasterTex papers, respectively,

followed by sonication in ethanol for 5 min and deionized water for 10 min. It is important to mention that the polishing effect on the BDD electrode is less effective compared to other materials such as gold, platinum, copper, etc. Nevertheless, we have noticed that the polishing can clean the BDD electrode and this practice has repeatedly been used in our labs as exemplified by our previous publications [14-17, 19]. For electroanalysis in ACN, TBAH, a quaternary ammonium salt, serves mainly used as an electrolyte. The salt consists positively charged tetrabutylammonium and weakly basic hexafluorophosphate anion. Such chemically inert species allows the salt to serve as an inert electrolyte over a wide potential range, particularly with the BDD electrode in ACN.

2.3 The growth of *Escherichia coli*

The microorganism was grown shaking (150 rpm) in LB (Luria-Bertani) medium without/with 5 mM exogenous TRP at 37 ˚C. This nutritionally rich medium is routinely used to grow bacterial cultures. LB broth contains (per mL), 10 mg tryptone (a mixture of peptides formed by the digestion of casein with the pancreatic enzyme, trypsin), 5 mg yeast extract (an autolysate of yeast cells), and 5 mg NaCl. The whole-cell cultures are used for the monitoring study. For the monitoring the production of indole, sample aliquots are taken at different time intervals (4, 6, and 8 h). For the *E. coli* bacterial culture without addition of TRP, a sample aliquot was taken at 8 h. The *E. coli* was grown is an aqueous media. Then, the bacterial culture was diluted 100 times while the bacterial culture without TRP was diluted 50 times in 0.2 M TBAH/ACN. For the Kovac's test, sample aliquots are taken at 8 and 30 h.

3. Results and discussion

3.1 Electrochemical characteristics of indole and tryptophan in aqueous media

As an aromatic heterocyclic compound, indole consists of a benzene ring fused to a pyrrole ring. The C3 position of the pyrrole ring is more susceptible to substitution. Therefore, most indole derivatives, e.g., TRP, indole propionic acid, and indole acetic acid, have a corresponding substituent at this position. The electrochemical oxidation of indole in aqueous media was previously investigated. In brief, the oxidation of indole is pH-dependent above pH 3.3, and one electron is transferred following the liberation of a proton, whereas the oxidation of indole is pH-independent below pH 3.3 and only an electron is transferred [23, 24].

In our initial attempts using indole and TRP (in aqueous media), similar characteristics were observed. Electrochemical oxidation of indole at pH 2 and pH 7 gave cyclic voltammograms (CVs) with a broad peak at a low oxidation potential ~ + 0.9 V and a second peak at high oxidation potential ~ + 1.5 V. The peak of indole diminished rapidly after the second scan and shifted to less positive values (**Fig. 1a, c**). The electrochemical behavior of TRP in the aqueous media was similar to indole (**Fig. S1a, c**). The results obtained here suggested the forming of polymer film on the surface on the BDD electrode after a subsequent run of CVs at pH 2 and pH 7.

We suspect the electrochemical (EC) oxidation mechanism of indole and TRP in aqueous media is that the nucleophilic attack of water on the radical formed in the first oxidation step was capable of rapidly hydroxylating the indole molecule as also suggested by Enache and

Oliveira-Brett [24]. The hydroxylated indole was then subject to further oxidation involving the formation of a number of other plausible oxidation products.

The most prominent oxidation product might well be 7-hydroxyindole [25]. A plausible pathway for the electrochemical oxidation of indole and TRP in aqueous media is suggested in **Scheme 1.** The broad oxidation peak ~ + 1.5 V observed at pH 2 and pH 7 could be attributed to the collective oxidation of indoles and higher oxidized derivatives.

The DPVs of indole obtained at pH 2 and pH 7 also showed one single peak at ~ + 0.7 V with diminishing magnitude after the second and third scan, likely due to the adsorption of oxidation products and subsequent electrode fouling (**Fig. 1b, d**). The DPVs behavior of TRP obtained at pH 2 and pH 7 was similar to indole (**Fig. S1b, d**)

Interestingly, the DPV for the indole and TRP mixture at pH 2 and pH 7 revealed only one oxidation peak (**Fig. 2**), because the oxidation potential of indole and TRP is similar at pH 2 and pH 7.

3.2 Electrochemical behavior of Indole in non-aqueous media

Overall, we suspected water in our aqueous media was acting to hydroxylate indole and TRP, resulting in hydroxyindoles which bound and fouled the electrode surface. Thus, we turned our attention to non-aqueous media.

The electrochemical characteristics of indole in the non-aqueous medium were then investigated in 0.2 M TBAH/ACN using the bare BDD electrode. The CV obtained for indole exhibited one single irreversible peak at + 1.17 V, followed by a very broad peak during the first scan (**Fig. 3a**). The subsequent CV runs of indole (~ + 0.5 V to + 2 V) can result in the formation of a weak polyindole film on the surface of the BDD electrode. As discussed in section 3.2, the CV of indole in non-aqueous media shows one oxidation peak at +1.17 V followed by a very broad peak at higher potential due to the further oxidation of the first peak at +1.17 V (**Fig. 3a**). While for DPV, the scan was stopped at +1.5 V and did not go further to a higher potential which minimized further oxidation of indole products which might form a polymer (**Fig. 3b**). The indole oxidation peak occurred at a higher potential, decreased modestly with subsequent scans, but became stable after 10 cycles of repeated scanning. Similar behavior was observed with 1 mM indole for 10 repeated cycles. When the electrode was subject to a fresh 0.2 M TBAH/ACN solution, an electroactive peak at + 1.2 V was observed. The peak was not stable and decreased rapidly with repeated scanning (**Fig. S2**). As shown in **Fig. 3**, the electrochemical oxidation of indole was carried out in non-aqueous media. Therefore it oxidized at higher potential compared to the aqueous media and electroanalysis of the organic solvent occurred at higher potential compared to water which results in the electrochemical oxidation at higher potential. Note also that the response current to $Fe(CN)_6^{3-/4-}$ of the resulting electrode was considerably lower compared to a clean BDD electrode. The peak was also very broad and shifted to a higher potential, implying the formation of a weak electroactive film on the electrode area (**Fig. S3**). Noticeably, radical cations formed close to the anode could diffuse away from the electrode surface in this condition. Remaining radicals would combine to form a polymer, particularly at high indole concentration (> 1 mM). The chain length of polyindole would increase as electrooxidation progressed, to cover the electrode's active surface area. Nevertheless, the film was easily delaminated from the BDD electrode by CV before each measurement.

The first DPV obtained for indole at a clean BDD showed a prominent oxidation peak, followed by a broad peak at a higher potential. The second peak could be attributed to the oxidation of an indole oxidation product, i.e., polyindole formed at the BDD surface during the first scan. There was a minimal change of the peak amplitude when the electrode was subject to the second and third scan, indicating minimal polymerization of indole radicals within this scanning period (**Fig. 3b**). Based on the voltammograms observed for the BDD electrode in 0.2 M TBAH/ACN and some pertinent literature information [25-28], a mechanism is suggested for the electrochemical oxidation of indole to form a polyindole film (**Scheme 2a**). A number of regioisomeric couplings to give multiple polyindoles are possible [29]. The Pt electrodes used as a comparison because it has been used for indole detection in non-aqueous media which is similar to our present work.

One consideration we had at this stage was the fate of the removed proton in a solvent such as ACN. Water is of course highly miscible in ACN and probably participates to some degree in hydrogen bonding (CN--H). The acid in acetonitrile will result in an acid-base equilibrium [30]. The interaction of ACN with trifluoromethanesulfonic acid is known and gives rise to a large number of products comprising both neutral and protonated ACN [31]. Also, ACN serves as a hydrogen-bond acceptor in the reactions of phenyl 2,4,6-trinitrophenyl ether with amines in benzene–acetonitrile mixtures [32]. Evaluation of such evidence leads to the possibility that ACN could accept the H+ liberated. An alternative scenario involves the adsorption of H+ onto the electrode, followed by the hydrogen evolution [33].

3.3 Electrochemical behavior of Tryptophan in non-aqueous media

As depicted in **Scheme 1**, TRP is an indole derivative with an α-carboxylic acid group at the 3-position. The structural differences (compared to indole) of TRP appeared to prevent minimum electropolymerization. Although the electrochemical oxidation of TRP in aqueous media has been investigated extensively in the literature [24-29, 34-40]. Based on our observations and literature precedent, a plausible mechanism for the electrochemical oxidation of TRP in ACN is suggested in **Scheme 2b**. The CVs of the TRP in 0.2 M TBAH/ACN show two oxidation peaks at ~ + 0.9 V and + 1.3 V. The oxidation potential of TRP remains stable after 10 cycles of repeated scanning (**Fig. S4a**). Also, the DPVs of 10 µM TRP displayed a small change in the peak current when the electrode was subjected to the second and third scans (**Fig. S4b**). The electrode after 10 cycles of 20 µM TRP in 0.2 M TBAH/ACN was tested in $Fe(CN)_6^{3-/4-}$ and the CVs showed that there is a slightly lower current compared to a clean BDD electrode, indicating minimal polymerization of TRP compared to indole (**Fig. S5**).

3.4 Simultaneous detection of Indole and Tryptophan

Considering the capability of the BDD in ACN to exhibit distinctive peaks of indole and TRP, we hoped that both biomolecules could be detected together. The TRP and indole were detected first individually and then a mixture of these two analytes was tested. The two peaks were distinguished by referring the oxidation potential for each. The DPV of TRP and indole detected individually is presented in **Fig. 4a, b**. The DPV was then performed on a mixture of TRP and indole (**Fig. 4c**). As expected, the mixture exhibited two peaks with some degree of overlap. If TRP was prepared in methanol, there was no noticeable effect of methanol on the electrochemical response or the potential window. The final methanol percentage presented in the final solution is 1.75 % (**Fig. 4**).

In contrast, only one single peak was noted when the experiment was performed in aqueous electrolytes at pH 2 and pH 7 (**Fig. 2**). Thus, 0.2 M TBAH/ACN was chosen as the optimum media for selective detection of indole and TRP. Consequently, the DPV in ACN was used to establish the calibration curves and detect indole and TRP during the growth of *E. coli*.

Notice also that the first oxidation potential of TRP was shifted by 0.03 V to less positive value while the oxidation potential of indole was shifted by 0.028 V to a higher positive value in the standard mixture compared to their individual values. The peak area of the first oxidation peak of TRP was slightly less by $0.11x10^{-6}$ in the standard mixture and the peak area of indole was also decreased by $0.48x10^{-6}$ in the standard mixture. The values of the oxidation potentials and the peak areas for the individual and the standard mixture were summarized in **Table S1**.

3.5 Calibration curve of Indole and Tryptophan

The DPVs of indole and TRP at different concentrations are shown in **Fig. 5** and the first DPV was taken for the calibration curve. For indole with a single peak, the peak area was integrated and correlated with concentration. The peak potential of indole was concentration-dependent and the peak area was increased with increasing concentration resulting in a slight shift of the potential (**Fig. 5a**). A limit of detection (LOD) of 0.5 µM and linearity up to 100 µM with a correlation coefficient of $R^2 = 0.931$ was obtained (**Fig. 5a**, inset). The LOD was established as the signal response observable at the lowest concentration over the background signal (S/N = 3). It should be noted that several literature reports claim very low LODs, based on the estimated slope of the calibration curve. The claimed LOD is often at least ten-fold below the lowest concentration used to establish the calibration curve. This method is generally unsatisfactory and the values are rarely achieved using "real-world" samples.

Similar results were estimated for TRP. However, the shoulder of the second peak was deconvoluted and subtracted from the total peak area (OriginPro, 2017, OriginLab). The correlation coefficient of the calibrated linear curve was $R^2 = 0.987$ with the final methanol percentage presented in the final solution was 0.07 –0.7 % (**Fig. 5b**). Thomas *et al.* [41] reported two linear dynamic ranges for TRP: 0.6–9.0 µM and 10.0–100.0 µM for the carbon paste electrode modified with MWCNTs using the drop cast method. The LOD was reported as $4.20 \pm 0.58 \times 10^{-7}$ M, about ten-fold below the lowest concentration used to test the electrode response. In reality, the electrode's response was very similar for both 0.5 µM and 1 µM of TRP as clearly reported in the paper.

Turning our attention to a biological sample, the calibration of indole and TRP in a bacterial growth medium (LB) is considered very challenging, since this complex matrix contains various proteins and other biomolecules (**Fig. 6** and insets). The final methanol percentage presented in the final solution was 0.35 –3.5 % (**Fig. 6b**). As expected, the DPV responses of both analytes in a spiked LB medium, were noticeably lower, with a detection limit of 22 and 4.28 µM for indole and TRP, respectively. Notice also that the oxidation signals of both indole and TRP in LB media were lower than ACN. The calibration curves of indole and TRP were also carried out in the LB media, and the curves show linearity, which illustrated the measurement was quantitative. After each measurement, the BDD electrode was cleaned in 0.5 M H_2SO_4.

From a practical aspect, fecal indole concentrations, for example, from healthy adults vary widely from 0.30 mM to 6.64 mM [4]. In the laboratory, enterotoxigenic *E. coli* strain

H10407 produces over 3.3 mM indole during a 24-h period in the presence of 5 mM TRP [4]. It appeared to us that the detection limit using BDD electrodes in our work would be sufficient for the analysis of indole in such biological samples. The plasma TRP concentrations in case of obsessive-compulsive disorder and major depressive disorder range from 50 to 70 µM [42], significantly higher than the LOD of the bare BDD electrode. However, it is present with two metabolites, 5-hydroxytryptophan, and serotonin at much lower concentrations (ng/mL) in patients affected with different forms of amenorrhea [43]. This opens up a new challenge for chemosensing, i.e., to target a minute quantity of these two molecules together with TRP.

3.6 Monitoring the level of Tryptophan and Indole during the growth of *E. coli*

As mentioned in the Experimental Section, 5 mM of TRP was added to the growth medium, and this added amount deserves a brief discussion here. In *E. coli*, the enzyme tryptophanase produces indole from TRP and the final yield of indole depends on the amount of exogenous TRP. The enzyme converts TRP into an equal amount of indole, up to almost 5 mM. The DPVs for the *E. coli* cell broth collected at 4, 6, and 8 h were shown in **Fig. 7**. As expected, the level of TRP decreased corresponding to increasing indole levels. These concentrations were estimated as ~ 4, 3, and 2 mM for TRP and ~ 0.45, 0.92, and 2.5 mM for indole in the cell culture at 4, 6, and 8 h, respectively. Moreover, the DPV recorded in the growth media without the addition of TRP is presented in **Fig. 7**. However, the potential of TRP and indole in *E. coli* was shifted slightly to less positive value by 0.03 V and 0.116 V, respectively compared to the value obtained using the standards. Also, the concentrations of TRP and indole in *E.coli* were determined by the standard addition method. Thus, the corresponding concentration consumption of TRP resulting from metabolism by *E. coli* were 1, 2, and 3 mM during the bacterial growth. It was also anticipated that an appreciable amount of TRP was conjugated with intracellular protein and not available for detection. Nevertheless, judging from the detection limit and its applicability in complex media, this chemosensing approach is remarkably efficient and applicable and will find applications in diversified and important bioprocesses and biological samples. In addition, *E. coli* grown in LB media supplemented with 5 mM TRP for 8 h and 30 h were tested with Kovac's reagent. As shown in **Fig. S6**, positive results were shown with the bacterial culture grown for 8 h and 30 h, whereas negative results were observed with the LB media alone, due to the absence of indole.

4. Conclusions

The simultaneous electrochemical detection of indole and TRP was attempted in both aqueous and non-aqueous media on the bare BDD electrode. The results show electroanalysis using the BDD electrode in ACN together with TBAH was capable of distinguishing the oxidation peaks of the indole and TRP mixture with a detection limit of 0.5 µM for both biomolecules. In contrast, the simultaneous detection of both analytes was not successful aqueous media because the oxidation potentials of indole and TRP are similar. Non-aqueous chemosensing with a broad potential window is more suitable for the analysis of the target analytes and alleviates electrode fouling compared to aqueous media. The sensing protocol was demonstrated for monitoring the levels of TRP decrease and indole increase during the growth of *E. coli* in a complex medium. The sensing approach with BDD also circumvented electrode fouling during the electrochemical oxidation of electropolymerizable targets as well as its exposure to a complex medium.

Acknowledgments

This research was financially supported by SFI/EI Technology Innovation Development Award (TIDA) (SFI/12/TIDA/B2405). FJR, GPM, and FOG acknowledge support from Enterprise Ireland (CF-2017-0757-P). FOG acknowledges the grants awarded by the European Commission (FP7-PEOPLE-2013-ITN, 607786; FP7-KBBE-2012-6, CP-TP-312184; FP7-KBBE-2012-6, 311975; OCEAN 2011-2, 287589; Marie Curie 256596; EU-634486), Science Foundation Ireland (SSPC-2, 12/RC/2275; 13/TIDA/B2625; 12/TIDA/B2411; 12/TIDA/B2405; 14/TIDA/2438; 15/TIDA/2977), the Department of Agriculture and Food (FIRM/RSF/CoFoRD; FIRM 08/RDC/629; FIRM 1/F009/MabS; FIRM 13/F/516), the Irish Research Council for Science, Engineering and Technology (PD/2011/2414; GOIPG/2014/647), the Health Research Board/Irish Thoracic Society (MRCG-2014-6), the Marine Institute (Beaufort award C2CRA 2007/082) and Teagasc (Walsh Fellowship 2013). JDG thanks the Science Foundation Ireland (08/SRC/B1412) for research funding of the Irish Separation Science Cluster (ISSC) under the Strategic Research Cluster Programme. GPM acknowledges supports by the Science Foundation Ireland (SFI/12/IP/1315, SFI/09/RFP/CHS2353, and SSPC2 12/RC/2275), the Irish Research Council (GOIPG/2013/336) and UCC for a Strategic Research Fund Ph.D. Studentship.

Appendix A. Supplementary data

Supplementary data to this article can be found at

References

[1] G.W. Gribble, Introduction, Indole ring synthesis, John Wiley & Sons, Ltd 2016, pp. 1-38.
[2] W.A. Newton, Y. Morino, E.E. Snell, Properties of crystalline tryptophanase, J. Biol. Chem. 240 (1965) 1211-1218.
[3] T. Bansal, D. Englert, J. Lee, M. Hegde, T.K. Wood, A. Jayaraman, Differential effects of epinephrine, norepinephrine, and indole on *Escherichia coli* O157:H7 chemotaxis, colonization, and gene expression, Infect. Immun. 75 (2007) 4597-4607.
[4] C. Darkoh, C. Chappell, C. Gonzales, P. Okhuysen, A rapid and specific method for the detection of indole in complex biological samples, Appl. Environ. Microbiol. 81 (2015) 8093-8097.
[5] J. Domka, J. Lee, T.K. Wood, YliH (BssR) and YceP (BssS) regulate *Escherichia coli* K-12 biofilm formation by influencing cell signaling, Appl. Environ. Microbiol. 72 (2006) 2449-2459.
[6] H. Hirakawa, Y. Inazumi, T. Masaki, T. Hirata, A. Yamaguchi, Indole induces the expression of multidrug exporter genes in *Escherichia coli*, Mol. Microbiol. 55 (2005) 1113-1126.
[7] J.H. Lee, J. Lee, Indole as an intercellular signal in microbial communities, FEMS Microbiol. Rev. 34 (2010) 426-444.
[8] I. Gonzalez-Burgos, E. Olvera-Cortes, A.R. Del Angel-Meza, A. Feria-Velasco, Serotonin involvement in the spontaneous alternation ability: a behavioral study in tryptophan-restricted rats, Neurosci. Lett. 190 (1995) 143-145.
[9] D.M. Richard, M.A. Dawes, C.W. Mathias, A. Acheson, N. Hill-Kapturczak, D.M. Dougherty, L-Tryptophan: basic metabolic functions, behavioral research and therapeutic indications, Int. J. Tryptophan Res. 2 (2009) 45-60.

[10] T. Bansal, R.C. Alaniz, T.K. Wood, A. Jayaraman, The bacterial signal indole increases epithelial-cell tight-junction resistance and attenuates indicators of inflammation, Proc. Natl. Acad. Sci. U.S.A. 107 (2010) 228-233.
[11] C.A. Gallagher, L.B. Hough, S.M. Keefner, A. Seyed-Mozaffari, S. Archer, S.D. Glick, Identification and quantification of the indole alkaloid ibogaine in biological samples by gas chromatography-mass spectrometry, Biochem. Pharmacol. 49 (1995) 73-79.
[12] J.W.H. Yong, L. Ge, W.S. Wong, Z. Ma, S.N. Tan, Analyses of indole compounds in sugar cane (saccharum officinarum l.) juice by high performance liquid chromatography and liquid chromatography-mass spectrometry after solid-phase extraction, Separations 4 (2017) 1-12.
[13] Y.H. Zhu, Y. Yang, Z.X. Zhou, G.R. Li, M. Jiang, C. Zhang, S.Q. Chen, Direct determination of free tryptophan contents in soy sauces and its application as an index of soy sauce adulteration, Food Chem 118 (2010) 159-162.
[14] A. Buzid, J.H.T. Luong, F.J. Reen, F. O'Gara, J.D. Glennon, G.P. McGlacken, Rapid electrochemical detection of *Pseudomonas aeruginosa* signaling molecules by boron-doped diamond electrode, Methods Mol. Biol. 1673 (2018) 107-116.
[15] A. Buzid, E.O. Muimhneachain, F.J. Reen, P.E. Hayes, L.M. Pardo, F. Shang, F. O'Gara, J. Sperry, J.H.T. Luong, J.D. Glennon, G.P. McGlacken, Synthesis and electrochemical detection of a thiazolyl-indole natural product isolated from the nosocomial pathogen *Pseudomonas aeruginosa*, Anal. Bioanal. Chem. 408 (2016) 6361-6367.
[16] A. Buzid, F.J. Reen, V.K. Langsi, E.Ó. Muimhneacháin, F. O'Gara, G.P. McGlacken, J.H.T. Luong, J.D. Glennon, Direct and rapid electrochemical detection of *Pseudomonas aeruginosa* quorum signaling molecules in bacterial cultures and cystic fibrosis sputum samples through cationic surfactant-assisted membrane disruption, ChemElectroChem 4 (2017) 533-541.
[17] A. Buzid, F. Shang, F.J. Reen, E.O. Muimhneachain, S.L. Clarke, L. Zhou, J.H.T. Luong, F. O'Gara, G.P. McGlacken, J.D. Glennon, Molecular signature of *Pseudomonas aeruginosa* with simultaneous nanomolar detection of quorum sensing signaling molecules at a boron-doped diamond electrode, Sci. Rep. 6 (2016) 30001.
[18] F. Shang, E.O. Muimhneachain, F.J. Reen, A. Buzid, F. O'Gara, J.H.T. Luong, J.D. Glennon, G.P. McGlacken, One step preparation and electrochemical analysis of IQS, a cell-cell communication signal in the nosocomial pathogen *Pseudomonas aeruginosa*, Bioorg. Med. Chem. Lett. 24 (2014) 4703-4707.
[19] L. Zhou, J.D. Glennon, J.H.T. Luong, F.J. Reen, F. O'Gara, C. McSweeney, G.P. McGlacken, Detection of the Pseudomonas Quinolone Signal (PQS) by cyclic voltammetry and amperometry using a boron doped diamond electrode, Chem. Commun. 47 (2011) 10347-10349.
[20] D.K. Belghiti, E. Scorsone, J. de Sanoit, P. Bergonzo, Simultaneous detection of indole and 3-methylindole using boron-doped diamond electrodes, Phys. Status Solidi 213 (2016) 2662-2671.
[21] J.S. Foord, A. Chatterjee, Electrochemical detection of indoles at diamond electrodes, Phys. Status Solidi 202 (2005) 2110-2115.
[22] Q. Wang, A. Vasilescu, P. Subramanian, A. Vezeanu, V. Andrei, Y. Coffinier, M.S. Li, R. Boukherroub, S. Szunerits, Simultaneous electrochemical detection of tryptophan and tyrosine using boron-doped diamond and diamond nanowire electrodes, Electrochem Commun 35 (2013) 84-87.
[23] J. Bunnett, R. Jones, Names for hydrogen atoms, ions, and groups, and for reactions involving them (Recommendations 1988), Pure Appl. Chem. 60 (1988) 1115-1116.
[24] T.A. Enache, A.M. Oliveira-Brett, Pathways of electrochemical oxidation of indolic compounds, Electroanalysis 23 (2011) 1337-1344.

[25] K. Somers, E. Kryachko, A. Ceulemans, Theoretical study of indole: protonation, indolyl radical, tautomers of indole, and its interaction with water, Chem. Phys. 301 (2004) 61-79.
[26] K.M. Choi, J.H. Jang, H.W. Rhee, K.H. Kim, A study of polyindole perchlorate (PIP) prepared by electropolymerization, J. Appl. Polym. Sci. 46 (1992) 1695-1706.
[27] K.M. Choi, C.Y. Kim, K.H. Kim, Polymerization mechanism and physicochemical properties of electrochemically prepared polyindole tetrafluoroborate, J. Phys. Chem. A 96 (1992) 3782-3788.
[28] R.J. Waltman, A. Diaz, J. Bargon, Substituent effects in the electropolymerization of aromatic heterocyclic compounds, J. Phys. Chem. 88 (1984) 4343-4346.
[29] M. Saraji, A. Bagheri, Electropolymerization of indole and study of electrochemical behavior of the polymer in aqueous solutions, Synth. Met. 98 (1998) 57-63.
[30] M. Kilpatrick, M.L. Kilpatrick, Relative acid strengths in acetonitrile, Chem. Rev. 13 (1933) 131-137.
[31] G.E. Salnikov, A.M. Genaev, V.G. Vasiliev, V.G. Shubin, Interaction of acetonitrile with trifluoromethanesulfonic acid: unexpected formation of a wide variety of structures, Org. Biomol. Chem. 10 (2012) 2282-2288.
[32] O. Banjoko, I.A. Babatunde, Catalytic effects of hydrogen-bond acceptor solvent on nucleophilic aromatic substitution reactions in non-polar aprotic solvent: reactions of phenyl 2, 4, 6-trinitrophenyl ether with amines in benzene–acetonitrile mixtures, Tetrahedron 61 (2005) 8035-8040.
[33] M.N. Jackson, Y. Surendranath, Donor-dependent kinetics of interfacial proton-coupled electron transfer, J. Am. Chem. Soc. 138 (2016) 3228-3234.
[34] V. Brabec, V. Mornstein, Electrochemical behaviour of proteins at graphite electrodes: II. Electrooxidation of amino acids, Biophys. Chem. 12 (1980) 159-165.
[35] M.R.M. Domingues, P. Domingues, A. Reis, C. Fonseca, F.M. Amado, A.J. Ferrer-Correia, Identification of oxidation products and free radicals of tryptophan by mass spectrometry, J. Am. Soc. Mass Spectrom. 14 (2003) 406-416.
[36] B. Malfoy, J. Reynaud, Electrochemical investigations of amino acids at solid electrodes: part II. Amino acids containing no sulfur atoms: tryptophan, tyrosine, histidine and derivatives, J. Electroanal. Chem. Interfac. 114 (1980) 213-223.
[37] N. Nguyen, M.Z. Wrona, G. Dryhurst, Electrochemical oxidation of tryptophan, J. Electroanal. Chem. Interfac. 199 (1986) 101-126.
[38] C.J. Nielsen, R. Stotz, G.T. Cheek, R.F. Nelson, The anodic oxidation of indole in acetonitrile an anomalous product, J. Electroanal. Chem. Interfac. 90 (1978) 127-130.
[39] P. Pandey, R. Prakash, Electrochemical synthesis of polyindole and its evaluation for rechargeable battery applications, J. Electrochem. Soc. 145 (1998) 999-1003.
[40] L. Shagun, I. Dorofeev, V. Smirnov, I. Tokareva, M. Voronkov, Synthesis of poly (2, 2′, 3, 3′-indole), Russ. Chem. Bull. 61 (2012) 2360-2362.
[41] T. Thomas, R.J. Mascarenhas, O.J. D'Souza, P. Martis, J. Dalhalle, B.E. Swamy, Multi-walled carbon nanotube modified carbon paste electrode as a sensor for the amperometric detection of L-tryptophan in biological samples, J. Colloid Interface Sci. 402 (2013) 223-229.
[42] L. Bellodi, S. Erzegovesi, L. Bianchi, V. Lucini, R. Conca, A. Lucca, Plasma tryptophan levels and tryptophan/neutral amino acid ratios in obsessive-compulsive patients with and without depression, Psychiatry Res. 69 (1997) 9-15.
[43] A. Tagliamonte, G. Biggio, L. Vargiu, G.L. Gessa, Free tryptophan in serum controls brain tryptophan level and serotonin synthesis, Life Sci. 12 (1973) 277-287.

Fig. 1. CVs (a, b) were obtained for 10 continuous cycles of 20 µM indole whereas differential pulse voltammetry (DPVs) (b, d) of 10 µM indole were recorded for three repeated runs on bare BDD electrode vs. Ag/AgCl. (a) and (b) using 50 mM phosphate buffer, pH 2 with 20 % acetonitrile , ACN (80: 20, v/v) whereas (c) and (d) using 50 mM phosphate buffer, pH 7 with 20 % (ACN, 80: 20, v/v).

Scheme 1. Electrochemical oxidation of (a) indole and (b) tryptophan (TRP) in an aqueous medium.

Fig. 2. A mixture of 50 µM each of indole and TRP using (a) 50 mM phosphate buffer, pH 2 with 20 % ACN (80: 20, v/v) and (b) 50 mM phosphate buffer, pH 7 with 20 % ACN (80: 20, v/v) on the bare BDD electrode vs. Ag/AgCl.

Fig. 3. (a) CVs of 20 µM indole obtained for 10 continuous cycles and (b) DPVs of 10 µM indole recorded for three repeated runs on the bare BDD electrode vs. Ag/AgCl. The detection was achieved in 0.2 M tetrabutylammonium hexafluorophosphate (TBAH)/ACN.

Scheme 2. Electrochemical oxidation of (a) indole and (b) tryptophan in a non-aqueous medium.

Fig. 4. (a) DPVs of in the absence (dotted lines) and presence (solid lines) of 50 µM TRP, (b) DPV of 50 µM indole, and (c) a representative DPVs obtained for a mixture of TRP and indole (50 µM each). The detection was achieved on the bare BDD electrode using 0.2 M TBAH/ACN.

Fig. 5. (a) DPVs of different indole concentrations on the bare BDD electrode (1 µM –100 µM) and the calibration plot of indole (insert); intercept =7.84 x 10-7 ± µA and slope =1.64 x 10-7 ± µA/µM (95 % of confidence interval). (b) DPVs of different TRP concentrations on the bare BDD electrode (2 µM – 20 µM) and the calibration plot of TRP (insert); intercept = 1.85 x 10-7 ± µA and slope = 1.1 x 10-7 ± µA/µM (95% of confidence interval), using 0.2 M TBAH/ACN. The error bar was estimated from three different values of the signal response for each analyte concentration.

Fig. 6. Calibration curves of indole and TRP in LB media. (a) DPVs of different indole concentrations on the bare BDD electrode (10 µM –100 µM) and the calibration plot of indole in LB media (insert); intercept = -1.21 x 10-6 ± µA and slope = 8.4 x 10-8 ± µA/µM (95 % of confidence interval). (b) DPVs of different TRP concentrations on the bare BDD electrode (10 µM – 100 µM) and the calibration plot of TRP in LB media (insert); intercept = 7.5 x 10-7 ± µA and slope = 4.14 x 10-8 ± µA/µM (95% of confidence interval), using 0.2 M TBAH/ACN. A blank LB medium is the control presented as dotted lines. The error bar was estimated from three different values of the signal response for each analyte concentration.

Fig. 7. Monitoring the production of indole in the E. coli bacterial culture as a function of time and DPV of the E. coli bacterial culture grown for 8 h without the addition of TRP. The detection was achieved on the bare BDD electrode vs. Ag/AgCl.

1

2

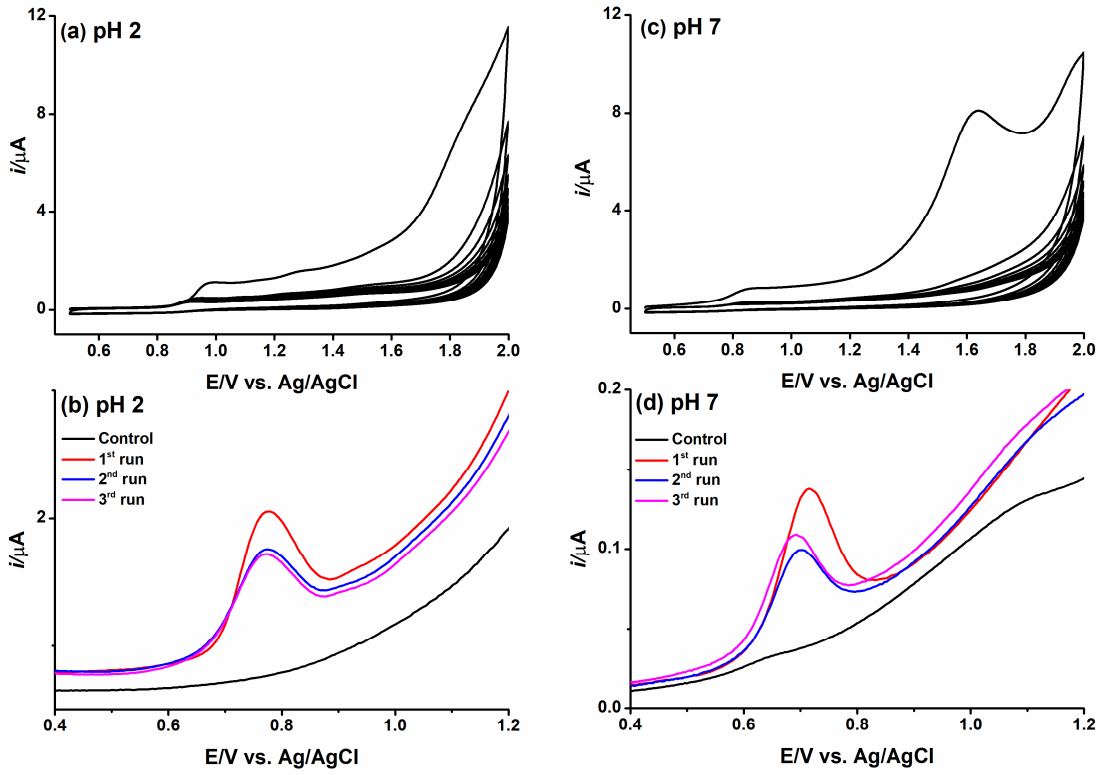

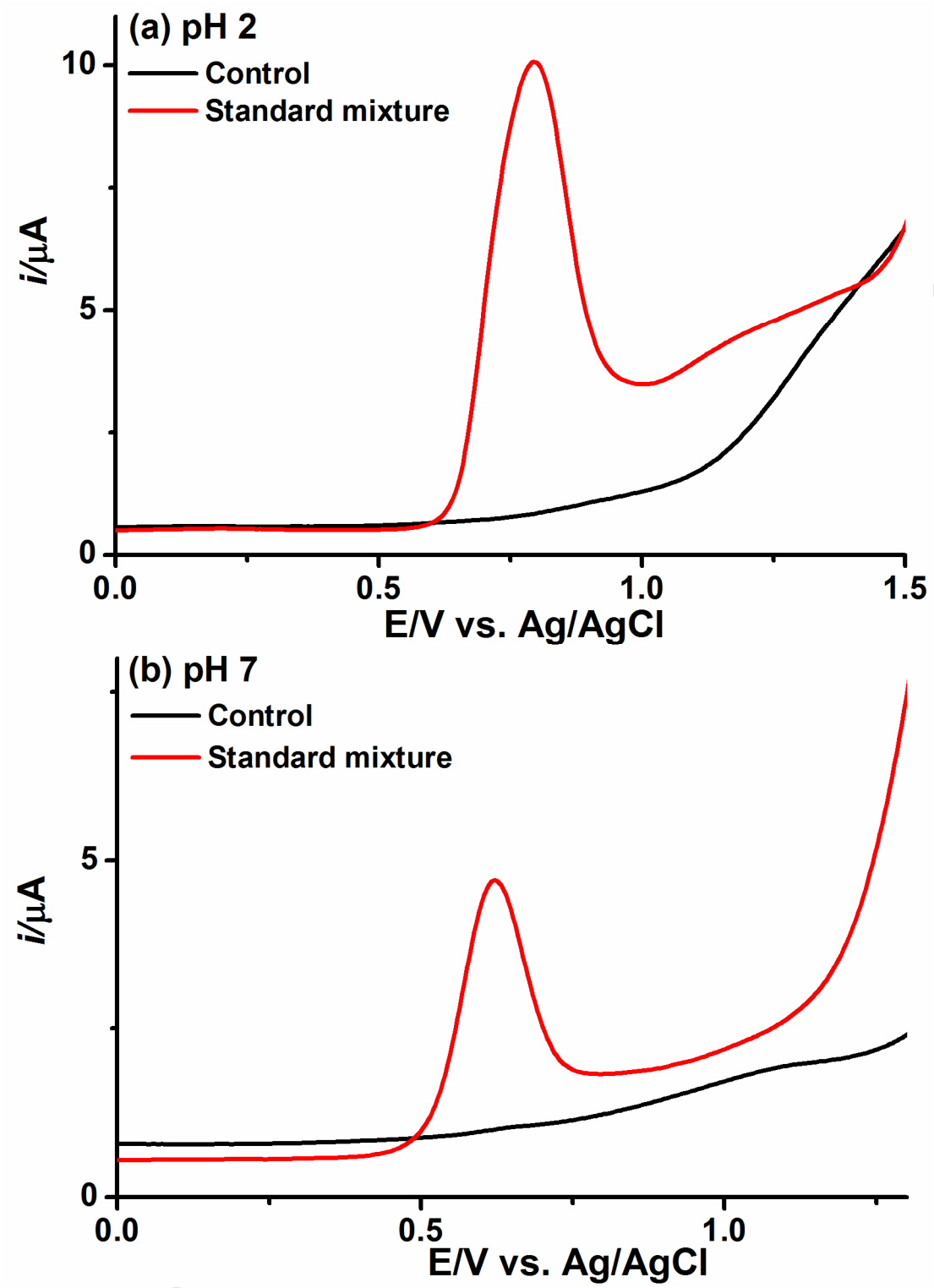
(a) pH 2
Control
Standard mixture
10
5
0
i/μA
0.0
0.5
1.0
1.5
E/V vs. Ag/AgCl
(b) pH 7
Control
Standard mixture
5
0
i/μA
0.0
0.5
1.0
E/V vs. Ag/AgCl

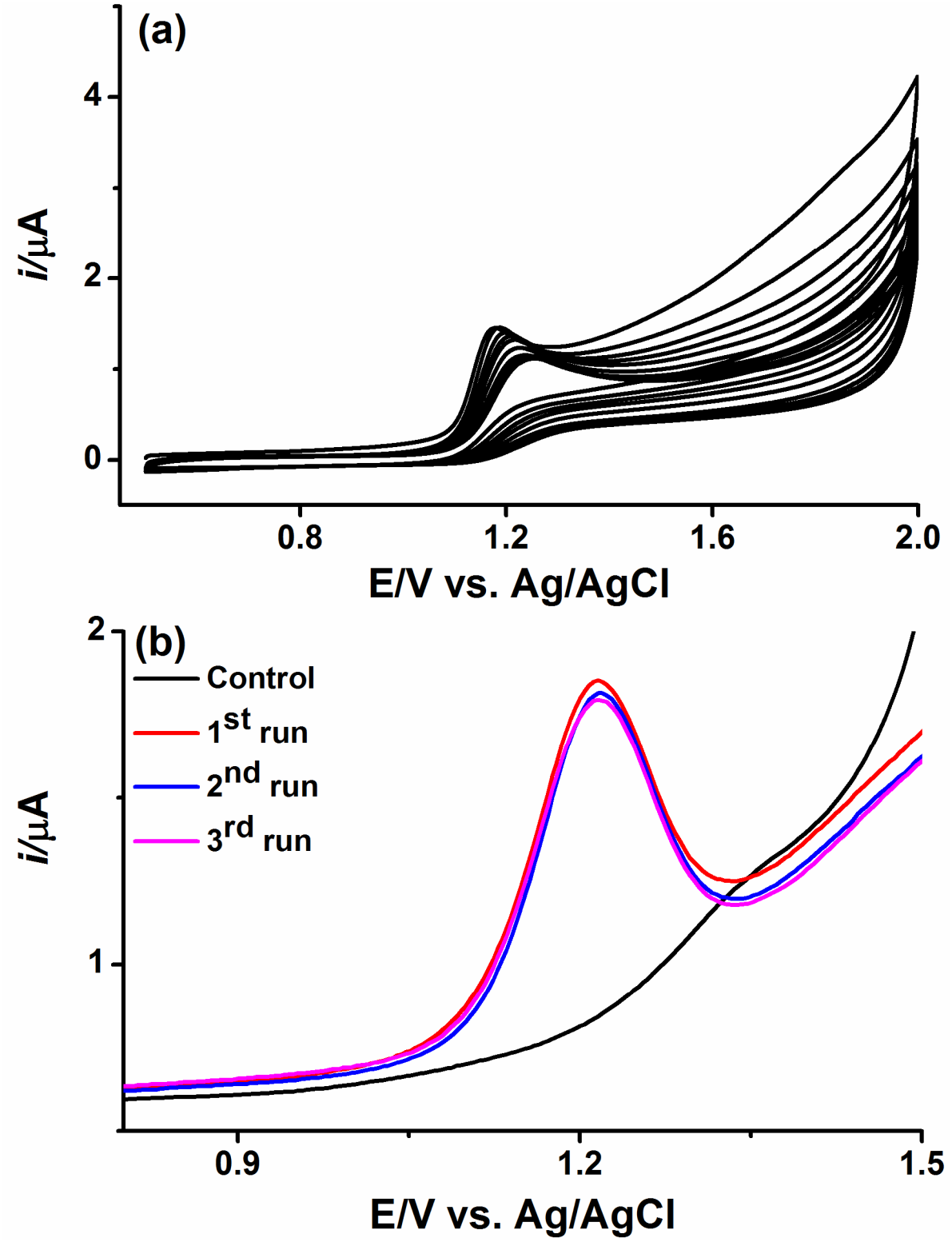
(a)
4
2
0
i/μA
0.8
1.2
1.6
2.0
E/V vs. Ag/AgCl
(b)
Control
1st run
2nd run
3rd run
2
1
i/μA
0.9
1.2
1.5
E/V vs. Ag/AgCl

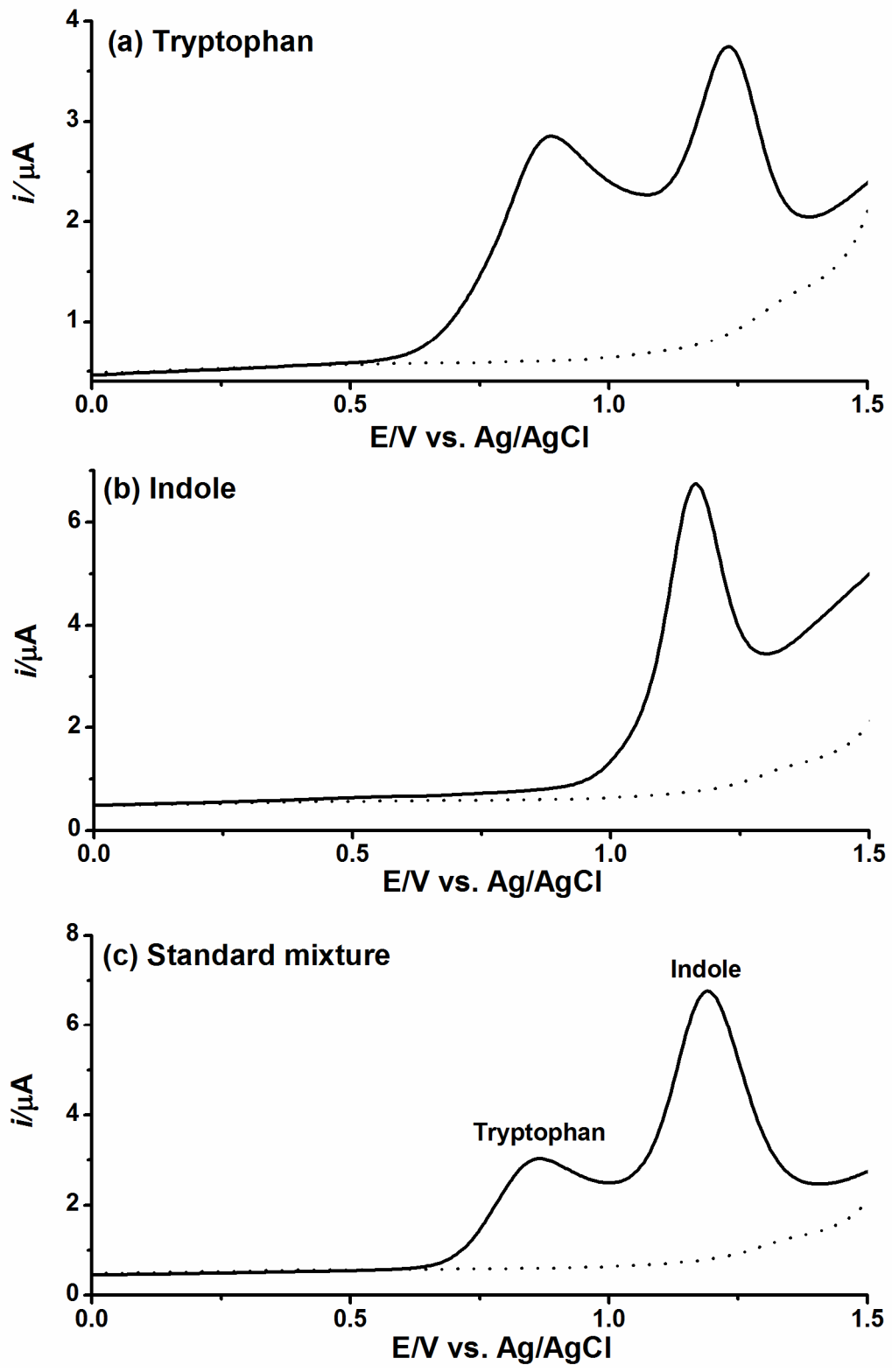
(a) Tryptophan
i/μA
E/V vs. Ag/AgCl
(b) Indole
i/μA
E/V vs. Ag/AgCl
(c) Standard mixture
Indole
Tryptophan
i/μA
E/V vs. Ag/AgCl

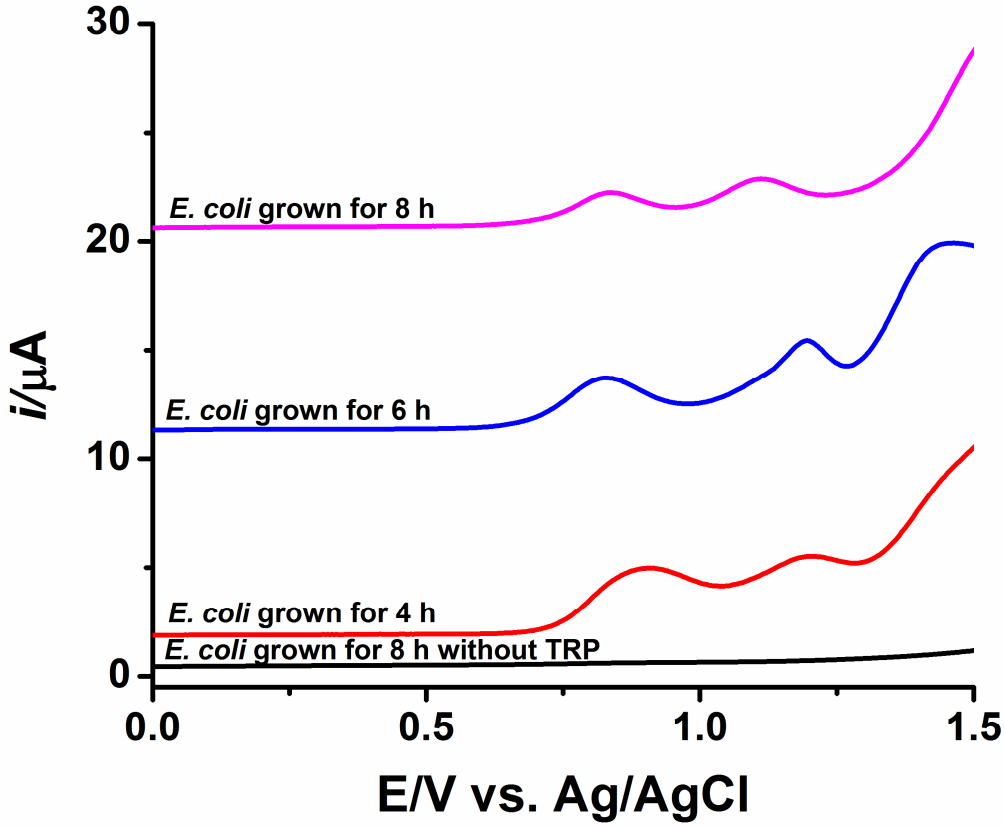

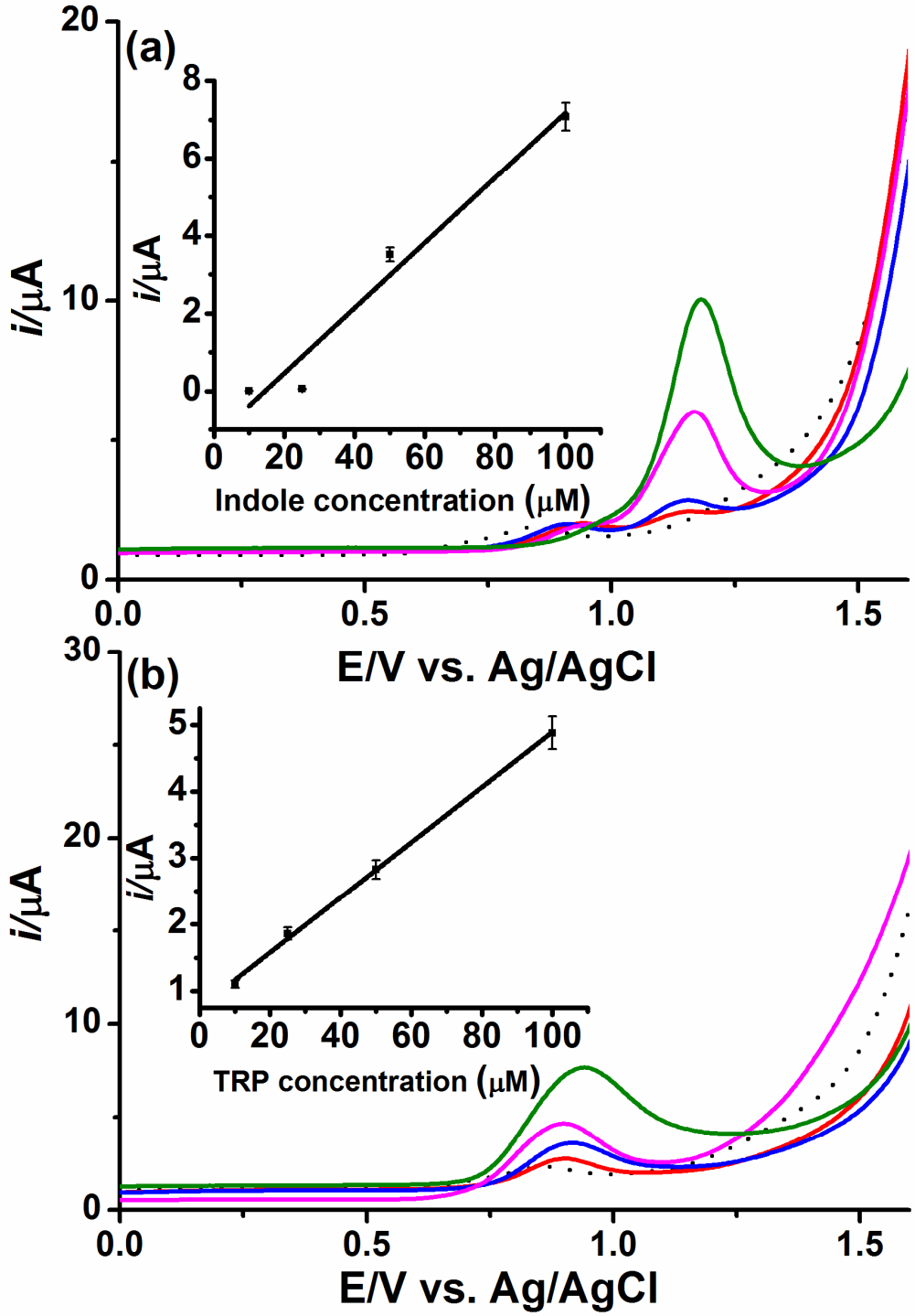
(a)
i/μA
E/V vs. Ag/AgCl
Indole concentration (μM)
(b)
i/μA
E/V vs. Ag/AgCl
TRP concentration (μM)

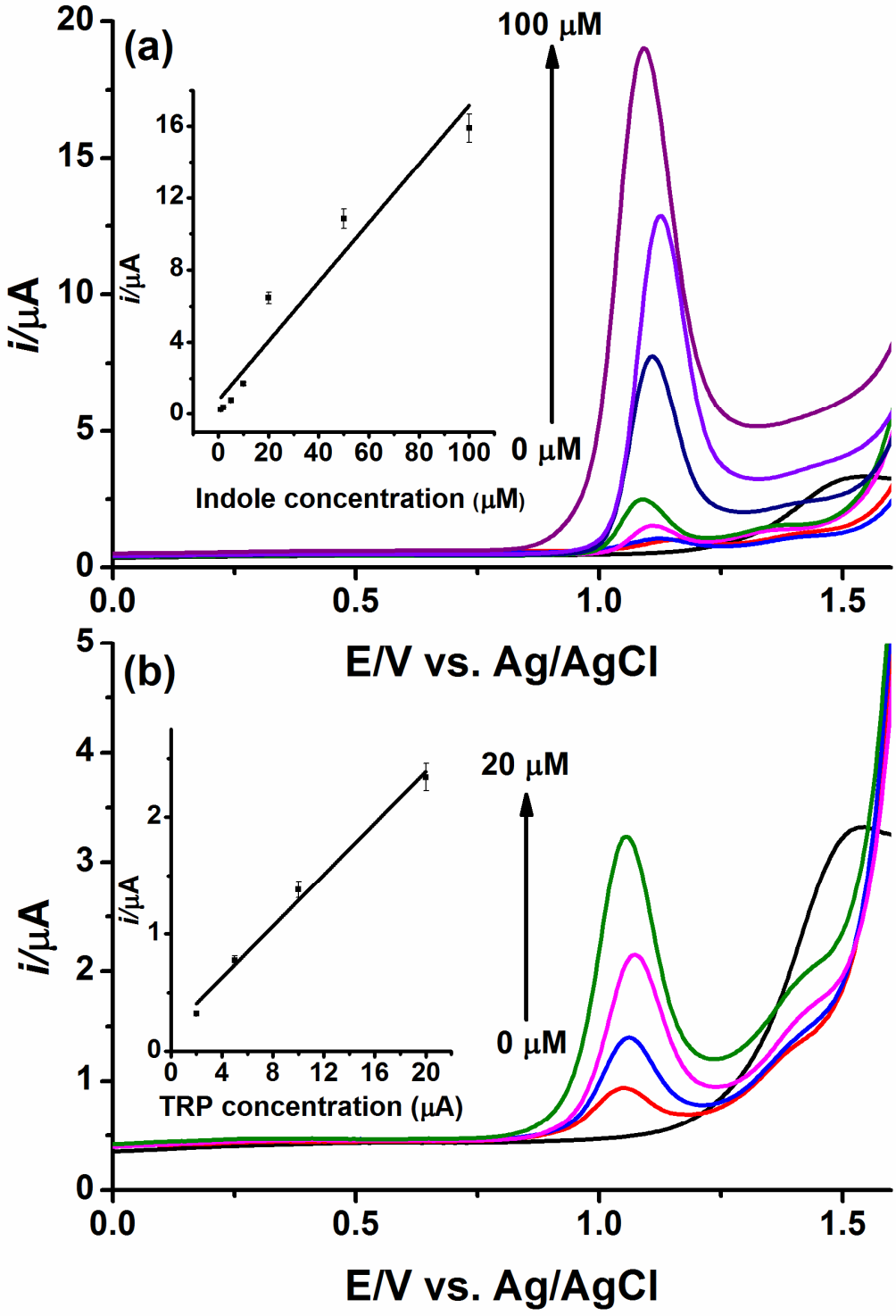
(a)
100 μM
0 μM
i/μA
Indole concentration (μM)
E/V vs. Ag/AgCl
(b)
20 μM
0 μM
i/μA
TRP concentration (μA)
E/V vs. Ag/AgCl